



Precision measurement of the Ξ_{cc}^{++} mass

LHCb collaboration[†]

Abstract

A measurement of the Ξ_{cc}^{++} mass is performed using data collected by the LHCb experiment between 2016 and 2018 in pp collisions at a centre-of-mass energy of 13 TeV, corresponding to an integrated luminosity of 5.6 fb^{-1} . The Ξ_{cc}^{++} candidates are reconstructed via the decay modes $\Xi_{cc}^{++} \rightarrow \Lambda_c^+ K^- \pi^+ \pi^+$ and $\Xi_{cc}^{++} \rightarrow \Xi_c^+ \pi^+$. The result, $3621.55 \pm 0.23 \text{ (stat)} \pm 0.30 \text{ (syst)} \text{ MeV}/c^2$, is the most precise measurement of the Ξ_{cc}^{++} mass to date.

Published in JHEP 02 (2020) 049

© 2020 CERN for the benefit of the LHCb collaboration. CC-BY-4.0 licence.

[†]Authors are listed at the end of this paper.

1 Introduction

Baryons containing two charm quarks and a lighter quark are predicted by the quark model [1, 2] and provide an ideal system to study the dynamics of bound states of quarks. Observation of the Ξ_{cc}^{++} (ccu) baryon via decays to $\Lambda_c^+ K^- \pi^+ \pi^+$ and $\Xi_c^+ \pi^+$ final states has been reported by the LHCb collaboration [3, 4].¹ The Ξ_{cc}^{++} mass was measured by the LHCb collaboration to be 3621.24 ± 0.65 (stat) ± 0.31 (syst) MeV/ c^2 . Before the LHCb observation, theoretical calculations using quark models [5–7], bag models [8], the Faddeev method [9], quantum chromodynamics (QCD) sum rules [10–13], potential models [14] and lattice QCD [15–17] predicted the mass of this state in the range 3450–3750 MeV/ c^2 . Most of the predictions using quark models are around 3600 MeV/ c^2 while other methods have a larger spread. Theoretical calculations of the Ξ_{cc}^{++} mass [18–21] after the LHCb observation fall into a ± 20 MeV/ c^2 window around the experimental value measured by LHCb.

At present, the experimental uncertainty on the Ξ_{cc}^{++} mass is still large compared to that of the singly charmed baryons. This paper presents an updated measurement of the Ξ_{cc}^{++} mass using the decay modes $\Xi_{cc}^{++} \rightarrow \Lambda_c^+ (\rightarrow p K^- \pi^+) K^- \pi^+ \pi^+$ and $\Xi_{cc}^{++} \rightarrow \Xi_c^+ (\rightarrow p K^- \pi^+) \pi^+$. The analysis uses a data sample corresponding to an integrated luminosity of 5.6 fb^{-1} , collected by the LHCb experiment during 2016–2018 in pp collisions at a centre-of-mass energy of 13 TeV. This measurement supersedes the results reported on the Ξ_{cc}^{++} mass in Refs. [3, 4], which only use pp collision data at 13 TeV taken in 2016, corresponding to an integrated luminosity of 1.7 fb^{-1} .

2 Detector and simulation

The LHCb detector [22, 23] is a single-arm forward spectrometer covering the pseudo-rapidity range $2 < \eta < 5$, designed for the study of particles containing b or c quarks. The detector includes a high-precision tracking system consisting of a silicon-strip vertex detector surrounding the pp interaction region [24], a large-area silicon-strip detector located upstream of a dipole magnet with a bending power of about 4 Tm, and three stations of silicon-strip detectors and straw drift tubes [25, 26] placed downstream of the magnet. The tracking system provides a measurement of the momentum of charged particles with a relative uncertainty that varies from 0.5% at low momentum to 1.0% at 200 GeV/ c . The momentum scale is calibrated using samples of $B^+ \rightarrow J/\psi K^+$ and $J/\psi \rightarrow \mu^+ \mu^-$ decays collected concurrently with the data sample used for this analysis [27, 28]. The relative accuracy of this procedure is estimated to be 3×10^{-4} using samples of other fully reconstructed b -hadron, Υ and K_S^0 decays. The minimum distance of a track to a primary pp collision vertex (PV), the impact parameter (IP), is measured with a resolution of $(15 + 29/(p_T/\text{GeV}/c)) \mu\text{m}$, where p_T is the momentum component transverse to the beam axis. Different types of charged hadrons are distinguished using information from two ring-imaging Cherenkov detectors [29]. Photons, electrons and hadrons are identified by a calorimeter system consisting of scintillating-pad and preshower detectors, an electromagnetic and a hadronic calorimeter. Muons are identified by a system composed of alternating layers of iron and multiwire proportional chambers [30].

The online event selection is performed by a trigger [31], which consists of a hardware

¹The inclusion of charge conjugate modes is implied throughout this paper.

stage, based on information from the calorimeter and muon systems, followed by a software stage, which applies a full event reconstruction. In between the two software stages, an alignment and calibration of the detector is performed in near real-time [32]. This process allows the reconstruction of the Ξ_{cc}^{++} decays to be performed entirely in the software trigger, whose output is used as input to the present analysis.

Simulated samples are used to model the effects of the detector acceptance, optimise selections and verify the validity of the methods used in the measurement. In the simulation, pp collisions are generated using PYTHIA 8 [33] with a LHCb specific configuration [34]. The production of doubly charmed Ξ_{cc}^{++} baryons is simulated using the dedicated generator GENXICC2.0 [35]. Decays of hadrons are described by EVTGEN [36], in which final-state radiation is generated using PHOTOS [37]. The interaction of the generated particles with the detector, and its response, are implemented using the GEANT4 toolkit [38] as described in Ref. [39]. Sources of background, such as those from $\Xi_{cc}^{++} \rightarrow \Xi_c^{\prime+}(\rightarrow \Xi_c^+\gamma)\pi^+$ and $\Xi_{cc}^{++} \rightarrow \Xi_c^+\rho^+(\rightarrow \pi^+\pi^0)$, are studied using the fast simulation package RAPIDSIM [40].

3 Event selection

The reconstruction of $\Xi_{cc}^{++} \rightarrow \Lambda_c^+(\rightarrow pK^-\pi^+)K^-\pi^+\pi^+$ and $\Xi_{cc}^{++} \rightarrow \Xi_c^+(\rightarrow pK^-\pi^+)\pi^+$ decays is similar to that used in previous LHCb analyses [3,4]. Candidate $\Xi_c^+(\Lambda_c^+) \rightarrow pK^-\pi^+$ decays are reconstructed from three charged particles identified as a p , K^- and π^+ using information from the RICH detectors [29]. The charged particles are required to form a good-quality vertex and be inconsistent with originating from any PV. The $\Xi_c^+(\Lambda_c^+)$ candidate is then combined with one (three) additional charged particle(s) to form a $\Xi_{cc}^{++} \rightarrow \Xi_c^+\pi^+$ ($\Xi_{cc}^{++} \rightarrow \Lambda_c^+K^-\pi^+\pi^+$) decay candidate. These additional particles must form a good-quality vertex with the $\Xi_c^+(\Lambda_c^+)$ candidate, which is required to be upstream of the $\Xi_c^+(\Lambda_c^+)$ decay vertex. Each Ξ_{cc}^{++} candidate is required to have $p_T > 2 \text{ GeV}/c$ and to be consistent with originating from its associated PV. The associated PV is that with respect to which the Ξ_{cc}^{++} candidate has the smallest χ_{IP}^2 . The χ_{IP}^2 is defined as the difference in χ^2 of the PV fit with and without the particle in question. To avoid candidates including duplicated tracks, each track pair is required to have an opening angle larger than 0.5 mrad or a momentum difference larger than 5% of the minimum momentum of the track pair.

In order to improve the signal purity, multivariate classifiers are trained to separate signal from background. The choice of classifier algorithms is based on their performance for each decay mode. A classifier based on the Boosted Decision Tree (BDT) algorithm [41,42] implemented in the TMVA toolkit [43] is used for the $\Xi_{cc}^{++} \rightarrow \Lambda_c^+K^-\pi^+\pi^+$ mode, while a Multilayer Perceptron (MLP) algorithm [43] is used for the $\Xi_{cc}^{++} \rightarrow \Xi_c^+\pi^+$ mode. The BDT for the $\Xi_{cc}^{++} \rightarrow \Lambda_c^+K^-\pi^+\pi^+$ decay is trained with simulated signal events as a signal proxy and wrong-sign $\Lambda_c^+K^-\pi^+\pi^-$ combinations (3525–3725 MeV/ c^2) in data, where the two final-state pions have opposite charges, as a background proxy. Both the signal and background proxies are required to pass the selection described above. Variables associated with the Ξ_{cc}^{++} candidates used in the training include the vertex-fit quality, the χ_{IP}^2 , the angle between the momentum and the displacement vector, the flight-distance χ^2 between the PV and the decay vertex. The flight-distance χ^2 is defined as the χ^2 of the hypothesis that the decay vertex of the candidate coincides with its associated PV. Variables associated with the decay products of the Ξ_{cc}^{++} candidates (the Λ_c^+ , K^- and π^+)

used in the training include their p_T and χ_{IP}^2 , the vertex-fit quality of the Λ_c^+ candidates and the smallest p_T among the Λ_c^+ decay products (p , K^- and π^+). Particle-identification information for the final-state particles is also used.

The threshold applied to the classifier response is determined by maximising the signal significance $S/\sqrt{S+B}$, where S is the expected signal yield estimated using simulation, and B is the background yield evaluated in the upper sideband of data (3800–3900 MeV/ c^2) extrapolated to the signal region (3607–3635 MeV/ c^2). The multivariate classifier for the $\Xi_{cc}^{++} \rightarrow \Xi_c^+ \pi^+$ decay is developed following the same strategy as that for the $\Xi_{cc}^{++} \rightarrow \Lambda_c^+ K^- \pi^+ \pi^+$ decay.

After the full selection, an event may still contain more than one Ξ_{cc}^{++} candidate. According to studies on simulated decays and the wrong-sign control sample, multiple candidates in the same event may form a peaking structure in the mass distribution of the Ξ_{cc}^{++} candidates if they are obtained from the same final-state tracks, but via swapping two final state tracks (e.g. the K^- from the Λ_c^+ decay and the K^- from the Ξ_{cc}^{++} decay). In this case, one candidate is chosen randomly. Other kinds of multiple candidates, which account for 8% ($< 1\%$) of the $\Xi_{cc}^{++} \rightarrow \Lambda_c^+ K^- \pi^+ \pi^+$ ($\Xi_{cc}^{++} \rightarrow \Xi_c^+ \pi^+$) signal events, are not removed since they do not form a peaking background.

4 Mass measurement

To improve the mass resolution, the invariant mass of a Ξ_{cc}^{++} candidate is computed as

$$\begin{aligned} m_{\text{cand}}(\Xi_{cc}^{++}) &= m(\Lambda_c^+ K^- \pi^+ \pi^+) - m(\Lambda_c^+) + M_{\text{PDG}}(\Lambda_c^+), \\ m_{\text{cand}}(\Xi_{cc}^{++}) &= m(\Xi_c^+ \pi^+) - m(\Xi_c^+) + M_{\text{LHCb}}(\Xi_c^+), \end{aligned} \quad (1)$$

where $m(\Lambda_c^+ K^- \pi^+ \pi^+)$ and $m(\Xi_c^+ \pi^+)$ are the reconstructed Ξ_{cc}^{++} masses; $m(\Lambda_c^+)$ and $m(\Xi_c^+)$ are the reconstructed Λ_c^+ and Ξ_c^+ masses; $M_{\text{PDG}}(\Lambda_c^+)$ is the known value of the Λ_c^+ mass; $M_{\text{LHCb}}(\Xi_c^+)$ is the known value of the Ξ_c^+ mass. The known value of the Λ_c^+ mass is 2286.46 ± 0.14 MeV/ c^2 [44, 45], and that of the Ξ_c^+ mass is determined to be 2467.97 ± 0.22 MeV/ c^2 using $M_{\text{PDG}}(\Lambda_c^+)$ and the difference between $m(\Xi_c^+)$ and $m(\Lambda_c^+)$ of $181.51 \pm 0.14 \pm 0.10$ MeV/ c^2 measured by the LHCb collaboration [46].

The $m_{\text{cand}}(\Xi_{cc}^{++})$ mass distributions of the selected Ξ_{cc}^{++} candidates are shown in Fig. 1 for the $\Xi_{cc}^{++} \rightarrow \Lambda_c^+ K^- \pi^+ \pi^+$ and $\Xi_{cc}^{++} \rightarrow \Xi_c^+ \pi^+$ decay modes. The Ξ_{cc}^{++} mass is determined by performing unbinned extended maximum-likelihood fits to the two $m_{\text{cand}}(\Xi_{cc}^{++})$ mass distributions. The signal components are described by a modified Gaussian function with a power-law tail on the left-hand side of the distribution [47], parameterised as

$$f(x; \alpha, N, \bar{x}, \sigma) = \begin{cases} e^{-\frac{1}{2}(\frac{x-\bar{x}}{\sigma})^2} & \text{for } \frac{x-\bar{x}}{\sigma} > -\alpha \\ \left(\frac{N}{|\alpha|}\right)^N e^{-\frac{|\alpha|^2}{2}} \left(\frac{N}{|\alpha|} - |\alpha| - \frac{x-\bar{x}}{\sigma}\right)^{-N} & \text{for } \frac{x-\bar{x}}{\sigma} \leq -\alpha. \end{cases} \quad (2)$$

The peak position, \bar{x} , and width, σ , of the function are allowed to vary in the fit. The power-law tail parameters, N and α , are fixed from simulation. The background from randomly associated tracks is modelled using an exponential function. Background contributions from the partially reconstructed decays $\Xi_{cc}^{++} \rightarrow \Xi_c'^+ (\rightarrow \Xi_c^+ \gamma) \pi^+$ and $\Xi_{cc}^{++} \rightarrow \Xi_c^+ \rho^+ (\rightarrow \pi^+ \pi^0)$, where photons and neutral π^0 mesons are not reconstructed, can contribute to the $\Xi_{cc}^{++} \rightarrow \Xi_c^+ \pi^+$ decay mode. The mass line shapes of these partially reconstructed backgrounds are determined from simulation.

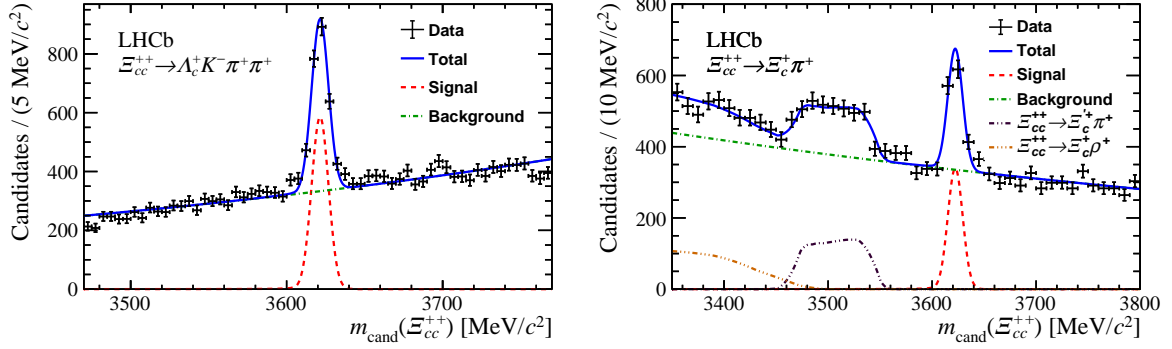


Figure 1: Invariant-mass distributions of (left) $\Xi_{cc}^{++} \rightarrow \Lambda_c^+ K^- \pi^+ \pi^+$ and (right) $\Xi_{cc}^{++} \rightarrow \Xi_c^+ \pi^+$ decay candidates, in the mass range of 3470–3770 MeV/c^2 and 3350–3800 MeV/c^2 , respectively. The results of unbinned extended maximum-likelihood fits to the mass distributions are indicated by the blue solid lines.

The fits return signal yields of 1598 ± 64 and 616 ± 47 for the $\Xi_{cc}^{++} \rightarrow \Lambda_c^+ K^- \pi^+ \pi^+$ and $\Xi_{cc}^{++} \rightarrow \Xi_c^+ \pi^+$ decay modes, respectively. The peak positions are determined with the $\Xi_{cc}^{++} \rightarrow \Lambda_c^+ K^- \pi^+ \pi^+$ and $\Xi_{cc}^{++} \rightarrow \Xi_c^+ \pi^+$ decay modes to be $3622.08 \pm 0.24 \text{ MeV}/c^2$ and $3622.37 \pm 0.60 \text{ MeV}/c^2$, respectively, where the uncertainty is statistical only.

Due to multiple scattering, the opening angle between the Ξ_{cc}^{++} decay products can be increased or decreased. This can bias both the resulting Ξ_{cc}^{++} mass and the measured decay length. Since the selection is more efficient for candidates with larger reconstructed decay lengths, and the decay length is correlated with the mass by the effect of the multiple scattering, this can bias the Ξ_{cc}^{++} mass measurement. This effect was studied with charmed hadrons, D^+ , D^0 , D_s^+ , Λ_c^+ , and was found to be well reproduced by simulation [3]. Corresponding corrections of $-0.61 \pm 0.09 \text{ MeV}/c^2$ for $\Xi_{cc}^{++} \rightarrow \Lambda_c^+ K^- \pi^+ \pi^+$ and $-0.45 \pm 0.09 \text{ MeV}/c^2$ for $\Xi_{cc}^{++} \rightarrow \Xi_c^+ \pi^+$ are determined using simulated candidates by comparing the fitted mass with signal candidates before and after applying the event selection. These corrections are applied to the fitted mass values. The uncertainties are due to the limited size of simulated samples, and are taken as the systematic uncertainties from the selection-induced bias on the Ξ_{cc}^{++} mass. The difference of the kinematic distributions in simulation and data is considered as a systematic uncertainty and is discussed in Sec. 5.

Low-momentum photons emitted by the final-state particles are not reconstructed. This distorts the reconstructed mass distribution and can bias the fitted mass value. This effect is studied with the simulation. To disentangle this effect from those due to reconstruction, the mass of the Ξ_{cc}^{++} candidates calculated with the true momenta of the final-state particles is smeared with different resolution values. The difference between the fitted and input mass values is studied as a function of the mass resolution, and the difference corresponding to the mass resolution in data is taken as a correction. Alternative signal models are also considered. The largest difference of the fitted mass with final-state radiation corrections between the nominal and the alternative is quoted as the uncertainty. Following the procedure described above, the corrections due to the final-state radiation are determined as $0.06 \pm 0.05 \text{ MeV}/c^2$ and $0.03 \pm 0.16 \text{ MeV}/c^2$ for the $\Xi_{cc}^{++} \rightarrow \Lambda_c^+ K^- \pi^+ \pi^+$ and $\Xi_{cc}^{++} \rightarrow \Xi_c^+ \pi^+$ decay modes, respectively. The uncertainties on the corrections are due to the limited size of the simulated samples, and the difference between the corrections with different signal models.

5 Systematic uncertainties

The dominant source of systematic uncertainty on the mass measurement is due to the momentum-scale calibration [27,28]. It amounts to $0.21 \text{ MeV}/c^2$ for the $\Xi_{cc}^{++} \rightarrow \Lambda_c^+ K^- \pi^+ \pi^+$ decay, and $0.34 \text{ MeV}/c^2$ for the $\Xi_{cc}^{++} \rightarrow \Xi_c^+ \pi^+$ decay due to larger Q -value. A further uncertainty arises from the correction for energy loss in the spectrometer, which is known with 10% accuracy [23]. This uncertainty was studied in Ref. [28], and amounts to $0.03 \text{ MeV}/c^2$ for $D^0 \rightarrow K^+ K^- \pi^+ \pi^-$ decays. The uncertainties on the Ξ_{cc}^{++} mass are scaled from that of the D^0 decay by the number of final-state particles, and are determined to be $0.05 \text{ MeV}/c^2$ and $0.03 \text{ MeV}/c^2$ for the $\Xi_{cc}^{++} \rightarrow \Lambda_c^+ K^- \pi^+ \pi^+$ and $\Xi_{cc}^{++} \rightarrow \Xi_c^+ \pi^+$ decays, respectively.

Differences between kinematic distributions in simulation and data are treated as sources of systematic uncertainties on the corrections due to the selection procedure. The kinematic variables used in the event selection that are found to affect the corrections are listed below: p_T of Ξ_{cc}^{++} candidates; the angle between the momentum and the displacement vector from the PV to the decay vertex of the Ξ_{cc}^{++} and Λ_c^+ (Ξ_c^+) candidates; the χ_{IP}^2 of Ξ_{cc}^{++} and Λ_c^+ (Ξ_c^+) candidates and their decay products; the BDT (MLP) response; and the particle identification information. The distributions of these variables in simulation are weighted to match those in data where the background is subtracted by means of the *sPlot* technique [48]. Then, the corrections obtained with the weights are compared to those without weights, and largest variations of the corrections are taken as systematic uncertainties, which are $0.09 \text{ MeV}/c^2$ and $0.05 \text{ MeV}/c^2$ for the $\Xi_{cc}^{++} \rightarrow \Lambda_c^+ K^- \pi^+ \pi^+$ and $\Xi_{cc}^{++} \rightarrow \Xi_c^+ \pi^+$ decays, respectively.

The uncertainty related to the background description is estimated by repeating the fits with alternative models which include first and second-order polynomial functions. For the $\Xi_{cc}^{++} \rightarrow \Lambda_c^+ K^- \pi^+ \pi^+$ decay, the fit with a second-order polynomial function has better fit quality, but returns identical fitted mass. The largest changes on the fitted mass value are found to be $0.01 \text{ MeV}/c^2$ and $0.04 \text{ MeV}/c^2$ for the $\Xi_{cc}^{++} \rightarrow \Lambda_c^+ K^- \pi^+ \pi^+$ and $\Xi_{cc}^{++} \rightarrow \Xi_c^+ \pi^+$ decays, respectively, which are assigned as systematic uncertainties.

The mass of Ξ_{cc}^{++} candidates also depends on the value of the known Λ_c^+ and Ξ_c^+ masses. The uncertainties on the Λ_c^+ mass and on the mass difference between the Ξ_c^+ and Λ_c^+ are propagated to the Ξ_{cc}^{++} mass measurement. The corresponding uncertainties on the Ξ_{cc}^{++} mass are $0.14 \text{ MeV}/c^2$ and $0.22 \text{ MeV}/c^2$ for the $\Xi_{cc}^{++} \rightarrow \Lambda_c^+ K^- \pi^+ \pi^+$ decay and the $\Xi_{cc}^{++} \rightarrow \Xi_c^+ \pi^+$ decay, respectively.

The sources of systematic uncertainty considered in this analysis are summarised in Table 1. When computing the total uncertainty, the uncertainty on the momentum-scale calibration of the Ξ_c^+ mass from Ref. [46] is assumed to be fully correlated to that of the Ξ_{cc}^{++} mass. The total systematic uncertainty is calculated by summing the individual sources of uncertainty in quadrature.

6 Results and summary

The resulting values of the Ξ_{cc}^{++} mass using the $\Xi_{cc}^{++} \rightarrow \Lambda_c^+ K^- \pi^+ \pi^+$ and $\Xi_{cc}^{++} \rightarrow \Xi_c^+ \pi^+$ decay modes are $3621.53 \pm 0.24 \pm 0.29 \text{ MeV}/c^2$, and $3621.95 \pm 0.60 \pm 0.49 \text{ MeV}/c^2$, respectively, including corrections and systematic uncertainties. The combination of the two measurements is performed using the Best Linear Unbiased Estimator (BLUE) [49,50].

Table 1: Systematic uncertainties on the Ξ_{cc}^{++} mass measurements using $\Xi_{cc}^{++} \rightarrow \Lambda_c^+ K^- \pi^+ \pi^+$ and $\Xi_{cc}^{++} \rightarrow \Xi_c^+ \pi^+$ decays. The total systematic uncertainty on each mode is calculated by summing the individual sources of uncertainty in quadrature, except for the uncertainty on the momentum-scale calibration of the Ξ_c^+ mass [46], that is added linearly to that of the Ξ_{cc}^{++} mass.

Source	Uncertainty [MeV/c ²]	
	$\Xi_{cc}^{++} \rightarrow \Lambda_c^+ K^- \pi^+ \pi^+$	$\Xi_{cc}^{++} \rightarrow \Xi_c^+ \pi^+$
Momentum-scale calibration	0.21	0.34
Energy-loss correction	0.05	0.03
Simulation/data agreement	0.09	0.05
Selection-induced bias on the Ξ_{cc}^{++} mass	0.09	0.09
Final-state radiation	0.05	0.16
Background model	0.01	0.04
Λ_c^+ , Ξ_c^+ mass	0.14	0.22
Total	0.29	0.49

The combined Ξ_{cc}^{++} mass is determined to be

$$3621.55 \pm 0.23 \text{ (stat)} \pm 0.30 \text{ (syst)} \text{ MeV}/c^2.$$

In the combination, the correlation between the Λ_c^+ and Ξ_c^+ masses [45, 46] is taken into account. Uncertainties arising from the momentum-scale calibration, energy-loss corrections, and final-state radiation are assumed to be 100% correlated while other sources of systematic uncertainty are assumed to be uncorrelated. The individual mass measurements and the resulting combination are illustrated in Fig. 2. The averaged mass is dominated by the result for the $\Xi_{cc}^{++} \rightarrow \Lambda_c^+ K^- \pi^+ \pi^+$ mode, due to its larger yield and smaller momentum-scale uncertainty relative to that of the $\Xi_{cc}^{++} \rightarrow \Xi_c^+ \pi^+$ decay. This is the most precise measurement of the Ξ_{cc}^{++} mass to date, improving upon the previous weighted average mass value of $3621.24 \pm 0.65 \text{ (stat)} \pm 0.31 \text{ (syst)} \text{ MeV}/c^2$ from Ref. [4].

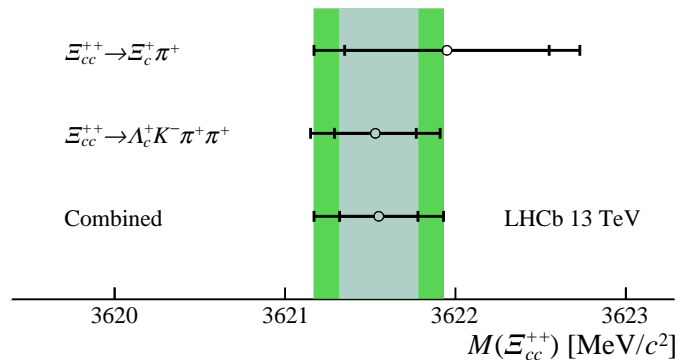


Figure 2: Measured Ξ_{cc}^{++} mass values and uncertainties obtained with the decay modes $\Xi_{cc}^{++} \rightarrow \Lambda_c^+ K^- \pi^+ \pi^+$ and $\Xi_{cc}^{++} \rightarrow \Xi_c^+ \pi^+$. The combination is performed using the best linear unbiased estimator [49, 50]. The inner error bars represent statistical uncertainties and the outer error bars represent the quadratic sum of statistical and systematic uncertainties. The inner and outer green bands correspond to the uncertainties on the averaged value.

Acknowledgements

We thank Chao-Hsi Chang, Cai-Dian Lü, Xing-Gang Wu, and Fu-Sheng Yu for the discussions on the production and decays of double-heavy-flavor baryons. We express our gratitude to our colleagues in the CERN accelerator departments for the excellent performance of the LHC. We thank the technical and administrative staff at the LHCb institutes. We acknowledge support from CERN and from the national agencies: CAPES, CNPq, FAPERJ and FINEP (Brazil); MOST and NSFC (China); CNRS/IN2P3 (France); BMBF, DFG and MPG (Germany); INFN (Italy); NWO (Netherlands); MNiSW and NCN (Poland); MEN/IFA (Romania); MSHE (Russia); MinECo (Spain); SNSF and SER (Switzerland); NASU (Ukraine); STFC (United Kingdom); DOE NP and NSF (USA). We acknowledge the computing resources that are provided by CERN, IN2P3 (France), KIT and DESY (Germany), INFN (Italy), SURF (Netherlands), PIC (Spain), GridPP (United Kingdom), RRCKI and Yandex LLC (Russia), CSCS (Switzerland), IFIN-HH (Romania), CBPF (Brazil), PL-GRID (Poland) and OSC (USA). We are indebted to the communities behind the multiple open-source software packages on which we depend. Individual groups or members have received support from AvH Foundation (Germany); EPLANET, Marie Skłodowska-Curie Actions and ERC (European Union); ANR, Labex P2IO and OCEVU, and Région Auvergne-Rhône-Alpes (France); Key Research Program of Frontier Sciences of CAS, CAS PIFI, and the Thousand Talents Program (China); RFBR, RSF and Yandex LLC (Russia); GVA, XuntaGal and GENCAT (Spain); the Royal Society and the Leverhulme Trust (United Kingdom).

References

- [1] M. Gell-Mann, *A schematic model of baryons and mesons*, Phys. Lett. **8** (1964) 214.
- [2] G. Zweig, *An SU_3 model for strong interaction symmetry and its breaking; Version 1*, Tech. Rep. CERN-TH-401, CERN, 1964; G. Zweig, *An SU_3 model for strong interaction symmetry and its breaking; Version 2*, Tech. Rep. CERN-TH-412, CERN, 1964.
- [3] LHCb collaboration, R. Aaij *et al.*, *Observation of the doubly charmed baryon Ξ_{cc}^{++}* , Phys. Rev. Lett. **119** (2017) 112001, [arXiv:1707.01621](#).
- [4] LHCb collaboration, R. Aaij *et al.*, *First observation of the doubly charmed baryon decay $\Xi_{cc}^{++} \rightarrow \Xi_c^+ \pi^+$* , Phys. Rev. Lett. **121** (2018) 162002, [arXiv:1807.01919](#).
- [5] D. Ebert, R. N. Faustov, V. O. Galkin, and A. P. Martynenko, *Mass spectra of doubly heavy baryons in the relativistic quark model*, Phys. Rev. **D66** (2002) 014008, [arXiv:hep-ph/0201217](#).
- [6] W. Roberts and M. Pervin, *Heavy baryons in a quark model*, Int. J. Mod. Phys. **A23** (2008) 2817, [arXiv:0711.2492](#).
- [7] M. Karliner and J. L. Rosner, *Baryons with two heavy quarks: Masses, production, decays, and detection*, Phys. Rev. **D90** (2014) 094007, [arXiv:1408.5877](#).

- [8] D. H. He *et al.*, *Evaluation of the spectra of baryons containing two heavy quarks in a bag model*, Phys. Rev. **D70** (2004) 094004, [arXiv:hep-ph/0403301](#).
- [9] A. Valcarce, H. Garcilazo, and J. Vijande, *Towards an understanding of heavy baryon spectroscopy*, Eur. Phys. J. **A37** (2008) 217, [arXiv:0807.2973](#).
- [10] Z. G. Wang, *Analysis of the $\frac{1}{2}^+$ doubly heavy baryon states with QCD sum rules*, Eur. Phys. J. **A45** (2010) 267, [arXiv:1001.4693](#).
- [11] V. V. Kiselev and A. K. Likhoded, *Baryons with two heavy quarks*, Phys. Usp. **45** (2002) 455, [arXiv:hep-ph/0103169](#).
- [12] J. R. Zhang and M. Q. Huang, *Doubly heavy baryons in QCD sum rules*, Phys. Rev. **D78** (2008) 094007, [arXiv:0810.5396](#).
- [13] T. M. Aliev, K. Azizi, and M. Savci, *Doubly Heavy Spin-1/2 Baryon Spectrum in QCD*, Nucl. Phys. **A895** (2012) 59, [arXiv:1205.2873](#).
- [14] J.-M. Richard and F. Stancu, *Double charm hadrons revisited*, Bled Workshops Phys. **6** (2005) 25, [arXiv:hep-ph/0511043](#).
- [15] R. Lewis, N. Mathur, and R. M. Woloshyn, *Charmed baryons in lattice QCD*, Phys. Rev. **D64** (2001) 094509, [arXiv:hep-ph/0107037](#).
- [16] UKQCD collaboration, J. M. Flynn, F. Mescia, and A. S. B. Tariq, *Spectroscopy of doubly charmed baryons in lattice QCD*, JHEP **07** (2003) 066, [arXiv:hep-lat/0307025](#).
- [17] L. Liu, H.-W. Lin, K. Orginos, and A. Walker-Loud, *Singly and doubly charmed $J=1/2$ baryon spectrum from lattice QCD*, Phys. Rev. **D81** (2010) 094505, [arXiv:0909.3294](#).
- [18] X. Z. Weng, X. L. Chen, and W. Z. Deng, *Masses of doubly heavy-quark baryons in an extended chromomagnetic model*, Phys. Rev. **D97** (2018) 054008, [arXiv:1801.08644](#).
- [19] Q. Li, C. H. Chang, S. X. Qin, and G. L. Wang, *The mass spectra and wave functions for the doubly heavy baryons with $J^P = 1^+$ heavy diquark core*, [arXiv:1903.02282](#).
- [20] Z. G. Wang, *Analysis of the doubly heavy baryon states and pentaquark states with QCD sum rules*, Eur. Phys. J. **C78** (2018) 826, [arXiv:1808.09820](#).
- [21] Q. F. Lü, K. L. Wang, L. Y. Xiao, and X. H. Zhong, *Mass spectra and radiative transitions of doubly heavy baryons in a relativized quark model*, Phys. Rev. **D96** (2017) 114006, [arXiv:1708.04468](#).
- [22] LHCb collaboration, A. A. Alves Jr. *et al.*, *The LHCb detector at the LHC*, JINST **3** (2008) S08005.
- [23] LHCb collaboration, R. Aaij *et al.*, *LHCb detector performance*, Int. J. Mod. Phys. **A30** (2015) 1530022, [arXiv:1412.6352](#).
- [24] R. Aaij *et al.*, *Performance of the LHCb Vertex Locator*, JINST **9** (2014) P09007, [arXiv:1405.7808](#).

- [25] R. Arink *et al.*, *Performance of the LHCb Outer Tracker*, JINST **9** (2014) P01002, arXiv:1311.3893.
- [26] P. d'Argent *et al.*, *Improved performance of the LHCb Outer Tracker in LHC Run 2*, JINST **12** (2017) P11016, arXiv:1708.00819.
- [27] LHCb collaboration, R. Aaij *et al.*, *Measurements of the Λ_b^0 , Ξ_b^- , and Ω_b^- baryon masses*, Phys. Rev. Lett. **110** (2013) 182001, arXiv:1302.1072.
- [28] LHCb collaboration, R. Aaij *et al.*, *Precision measurement of D meson mass differences*, JHEP **06** (2013) 065, arXiv:1304.6865.
- [29] M. Adinolfi *et al.*, *Performance of the LHCb RICH detector at the LHC*, Eur. Phys. J. **C73** (2013) 2431, arXiv:1211.6759.
- [30] A. A. Alves Jr. *et al.*, *Performance of the LHCb muon system*, JINST **8** (2013) P02022, arXiv:1211.1346.
- [31] R. Aaij *et al.*, *The LHCb trigger and its performance in 2011*, JINST **8** (2013) P04022, arXiv:1211.3055.
- [32] G. Dujany and B. Storaci, *Real-time alignment and calibration of the LHCb detector in Run II*, J. Phys. Conf. Ser. **664** (2015) 082010.
- [33] T. Sjöstrand, S. Mrenna, and P. Skands, *A brief introduction to PYTHIA 8.1*, Comput. Phys. Commun. **178** (2008) 852, arXiv:0710.3820.
- [34] I. Belyaev *et al.*, *Handling of the generation of primary events in Gauss, the LHCb simulation framework*, J. Phys. Conf. Ser. **331** (2011) 032047.
- [35] C. H. Chang, J. X. Wang, and X. G. Wu, *GENXICC2.0: An upgraded version of the generator for hadronic production of double heavy baryons Ξ_{cc} , Ξ_{bc} and Ξ_{bb}* , Comput. Phys. Commun. **181** (2010) 1144, arXiv:0910.4462; X. Y. Wang and X. G. Wu, *GENXICC2.1: An improved version of GENXICC for hadronic production of doubly heavy baryons*, Comput. Phys. Commun. **184** (2013) 1070, arXiv:1210.3458.
- [36] D. J. Lange, *The EvtGen particle decay simulation package*, Nucl. Instrum. Meth. **A462** (2001) 152.
- [37] P. Golonka and Z. Was, *PHOTOS Monte Carlo: A precision tool for QED corrections in Z and W decays*, Eur. Phys. J. **C45** (2006) 97, arXiv:hep-ph/0506026.
- [38] Geant4 collaboration, J. Allison *et al.*, *Geant4 developments and applications*, IEEE Trans. Nucl. Sci. **53** (2006) 270; Geant4 collaboration, S. Agostinelli *et al.*, *Geant4: A simulation toolkit*, Nucl. Instrum. Meth. **A506** (2003) 250.
- [39] M. Clemencic *et al.*, *The LHCb simulation application, Gauss: Design, evolution and experience*, J. Phys. Conf. Ser. **331** (2011) 032023.
- [40] G. A. Cowan, D. C. Craik, and M. D. Needham, *RapidSim: an application for the fast simulation of heavy-quark hadron decays*, Comput. Phys. Commun. **214** (2017) 239, arXiv:1612.07489.

- [41] L. Breiman, J. H. Friedman, R. A. Olshen, and C. J. Stone, *Classification and regression trees*, Wadsworth international group, Belmont, California, USA, 1984.
- [42] Y. Freund and R. E. Schapire, *A decision-theoretic generalization of on-line learning and an application to boosting*, J. Comput. Syst. Sci. **55** (1997) 119.
- [43] H. Voss, A. Hoecker, J. Stelzer, and F. Tegenfeldt, *TMVA — Toolkit for Multivariate Data Analysis with ROOT*, PoS **ACAT** (2007) 040; A. Hoecker *et al.*, *TMVA 4 — Toolkit for Multivariate Data Analysis with ROOT. Users Guide*, arXiv:physics/0703039.
- [44] BaBar collaboration, B. Aubert *et al.*, *A precision measurement of the Λ_c^+ baryon mass*, Phys. Rev. **D72** (2005) 052006, arXiv:hep-ex/0507009.
- [45] Particle Data Group, M. Tanabashi *et al.*, *Review of particle physics*, Phys. Rev. **D98** (2018) 030001, and 2019 update.
- [46] LHCb collaboration, R. Aaij *et al.*, *Precision measurement of the mass and lifetime of the Ξ_b^0 baryon*, Phys. Rev. Lett. **113** (2014) 032001, arXiv:1405.7223.
- [47] T. Skwarnicki, *A study of the radiative cascade transitions between the Upsilon-prime and Upsilon resonances*, PhD thesis, Institute of Nuclear Physics, Krakow, 1986, DESY-F31-86-02.
- [48] M. Pivk and F. R. Le Diberder, *sPlot: A statistical tool to unfold data distributions*, Nucl. Instrum. Meth. **A555** (2005) 356, arXiv:physics/0402083.
- [49] L. Lyons, D. Gibaut, and P. Clifford, *How to combine correlated estimates of a single physical quantity*, Nucl. Instrum. Meth. **A270** (1988) 110.
- [50] A. Valassi, *Combining correlated measurements of several different physical quantities*, Nucl. Instrum. Meth. **A500** (2003) 391.

LHCb collaboration

R. Aaij³¹, C. Abellán Beteta⁴⁹, T. Ackernley⁵⁹, B. Adeva⁴⁵, M. Adinolfi⁵³, H. Afsharnia⁹, C.A. Aidala⁸⁰, S. Aiola²⁵, Z. Ajaltouni⁹, S. Akar⁶⁶, P. Albicocco²², J. Albrecht¹⁴, F. Alessio⁴⁷, M. Alexander⁵⁸, A. Alfonso Alberro⁴⁴, G. Alkhazov³⁷, P. Alvarez Cartelle⁶⁰, A.A. Alves Jr⁴⁵, S. Amato², Y. Amhis¹¹, L. An²¹, L. Anderlini²¹, G. Andreassi⁴⁸, M. Andreotti²⁰, F. Archilli¹⁶, J. Arnau Romeu¹⁰, A. Artamonov⁴³, M. Artuso⁶⁷, K. Arzymatov⁴¹, E. Aslanides¹⁰, M. Atzeni⁴⁹, B. Audurier²⁶, S. Bachmann¹⁶, J.J. Back⁵⁵, S. Baker⁶⁰, V. Balagura^{11,b}, W. Baldini^{20,47}, A. Baranov⁴¹, R.J. Barlow⁶¹, S. Barsuk¹¹, W. Barter⁶⁰, M. Bartolini^{23,47,h}, F. Baryshnikov⁷⁷, G. Bassi²⁸, V. Batozskaya³⁵, B. Batsukh⁶⁷, A. Battig¹⁴, A. Bay⁴⁸, M. Becker¹⁴, F. Bedeschi²⁸, I. Bediaga¹, A. Beiter⁶⁷, L.J. Bel³¹, V. Belavin⁴¹, S. Belin²⁶, N. Bely⁵, V. Bellec⁴⁸, K. Belous⁴³, I. Belyaev³⁸, G. Bencivenni²², E. Ben-Haim¹², S. Benson³¹, S. Beranek¹³, A. Berezhnoy³⁹, R. Bernet⁴⁹, D. Berninghoff¹⁶, H.C. Bernstein⁶⁷, C. Bertella⁴⁷, E. Bertholet¹², A. Bertolin²⁷, C. Betancourt⁴⁹, F. Betti^{19,e}, M.O. Bettler⁵⁴, Ia. Bezshyiko⁴⁹, S. Bhasin⁵³, J. Bhom³³, M.S. Bieker¹⁴, S. Bifani⁵², P. Billoir¹², A. Bizzeti^{21,u}, M. Bjørn⁶², M.P. Blago⁴⁷, T. Blake⁵⁵, F. Blanc⁴⁸, S. Blusk⁶⁷, D. Bobulska⁵⁸, V. Bocci³⁰, O. Boente Garcia⁴⁵, T. Boettcher⁶³, A. Boldyrev⁷⁸, A. Bondar^{42,x}, N. Bondar³⁷, S. Borghi^{61,47}, M. Borisyak⁴¹, M. Borsato¹⁶, J.T. Borsuk³³, T.J.V. Bowcock⁵⁹, C. Bozzi²⁰, M.J. Bradley⁶⁰, S. Braun¹⁶, A. Brea Rodriguez⁴⁵, M. Brodski⁴⁷, J. Brodzicka³³, A. Brossa Gonzalo⁵⁵, D. Brundu²⁶, E. Buchanan⁵³, A. Buonauro⁴⁹, C. Burr⁴⁷, A. Bursche²⁶, J.S. Butter³¹, J. Buytaert⁴⁷, W. Byczynski⁴⁷, S. Cadeddu²⁶, H. Cai⁷², R. Calabrese^{20,g}, L. Calero Diaz²², S. Cali²², R. Calladine⁵², M. Calvi^{24,i}, M. Calvo Gomez^{44,m}, A. Camboni⁴⁴, P. Campana²², D.H. Campora Perez³¹, L. Capriotti^{19,e}, A. Carbone^{19,e}, G. Carboni²⁹, R. Cardinale^{23,h}, A. Cardini²⁶, P. Carniti^{24,i}, K. Carvalho Akiba³¹, A. Casais Vidal⁴⁵, G. Casse⁵⁹, M. Cattaneo⁴⁷, G. Cavallero⁴⁷, S. Celani⁴⁸, R. Cenci^{28,p}, J. Cerasoli¹⁰, M.G. Chapman⁵³, M. Charles^{12,47}, Ph. Charpentier⁴⁷, G. Chatzikonstantinidis⁵², M. Chefdeville⁸, V. Chekalina⁴¹, C. Chen³, S. Chen²⁶, A. Chernov³³, S.-G. Chitic⁴⁷, V. Chobanova⁴⁵, M. Chruszcz³³, A. Chubykin³⁷, P. Ciambrone²², M.F. Cicala⁵⁵, X. Cid Vidal⁴⁵, G. Ciezarek⁴⁷, F. Cindolo¹⁹, P.E.L. Clarke⁵⁷, M. Clemencic⁴⁷, H.V. Cliff⁵⁴, J. Closier⁴⁷, J.L. Cobbledick⁶¹, V. Coco⁴⁷, J.A.B. Coelho¹¹, J. Cogan¹⁰, E. Cogneras⁹, L. Cojocariu³⁶, P. Collins⁴⁷, T. Colombo⁴⁷, A. Comerma-Montells¹⁶, A. Contu²⁶, N. Cooke⁵², G. Coombs⁵⁸, S. Coquereau⁴⁴, G. Corti⁴⁷, C.M. Costa Sobral⁵⁵, B. Couturier⁴⁷, D.C. Craik⁶³, J. Crkovska⁶⁶, A. Crocombe⁵⁵, M. Cruz Torres¹, R. Currie⁵⁷, C.L. Da Silva⁶⁶, E. Dall'Occo¹⁴, J. Dalseno^{45,53}, C. D'Ambrosio⁴⁷, A. Danilina³⁸, P. d'Argent¹⁶, A. Davis⁶¹, O. De Aguiar Francisco⁴⁷, K. De Bruyn⁴⁷, S. De Capua⁶¹, M. De Cian⁴⁸, J.M. De Miranda¹, L. De Paula², M. De Serio^{18,d}, P. De Simone²², J.A. de Vries³¹, C.T. Dean⁶⁶, W. Dean⁸⁰, D. Decamp⁸, L. Del Buono¹², B. Delaney⁵⁴, H.-P. Dembinski¹⁵, M. Demmer¹⁴, A. Dendek³⁴, V. Denysenko⁴⁹, D. Derkach⁷⁸, O. Deschamps⁹, F. Desse¹¹, F. Dettori²⁶, B. Dey⁷, A. Di Canto⁴⁷, P. Di Nezza²², S. Didenko⁷⁷, H. Dijkstra⁴⁷, V. Dobishuk⁵¹, F. Dordei²⁶, M. Dorigo^{28,y}, A.C. dos Reis¹, L. Douglas⁵⁸, A. Dovbnya⁵⁰, K. Dreimanis⁵⁹, M.W. Dudek³³, L. Dufour⁴⁷, G. Dujany¹², P. Durante⁴⁷, J.M. Durham⁶⁶, D. Dutta⁶¹, R. Dzhelyadin^{43,†}, M. Dziewiecki¹⁶, A. Dziurda³³, A. Dzyuba³⁷, S. Easo⁵⁶, U. Egede⁶⁹, V. Egorychev³⁸, S. Eidelman^{42,x}, S. Eisenhardt⁵⁷, R. Ekelhof¹⁴, S. Ek-In⁴⁸, L. Eklund⁵⁸, S. Ely⁶⁷, A. Ene³⁶, E. Epple⁶⁶, S. Escher¹³, S. Esen³¹, T. Evans⁴⁷, A. Falabella¹⁹, J. Fan³, N. Farley⁵², S. Farry⁵⁹, D. Fazzini¹¹, P. Fedin³⁸, M. Féo⁴⁷, P. Fernandez Declara⁴⁷, A. Fernandez Prieto⁴⁵, F. Ferrari^{19,e}, L. Ferreira Lopes⁴⁸, F. Ferreira Rodrigues², S. Ferreres Sole³¹, M. Ferrillo⁴⁹, M. Ferro-Luzzi⁴⁷, S. Filippov⁴⁰, R.A. Fini¹⁸, M. Fiorini^{20,g}, M. Firlej³⁴, K.M. Fischer⁶², C. Fitzpatrick⁴⁷, T. Fiutowski³⁴, F. Fleuret^{11,b}, M. Fontana⁴⁷, F. Fontanelli^{23,h}, R. Forty⁴⁷, V. Franco Lima⁵⁹, M. Franco Sevilla⁶⁵, M. Frank⁴⁷, C. Frei⁴⁷, D.A. Friday⁵⁸, J. Fu^{25,q}, M. Fuehring¹⁴, W. Funk⁴⁷, E. Gabriel⁵⁷, A. Gallas Torreira⁴⁵, D. Galli^{19,e}, S. Gallorini²⁷, S. Gambetta⁵⁷, Y. Gan³, M. Gandelman², P. Gandini²⁵, Y. Gao⁴, L.M. Garcia Martin⁴⁶,

J. García Pardiñas⁴⁹, B. Garcia Plana⁴⁵, F.A. Garcia Rosales¹¹, J. Garra Tico⁵⁴, L. Garrido⁴⁴,
 D. Gascon⁴⁴, C. Gaspar⁴⁷, D. Gerick¹⁶, E. Gersabeck⁶¹, M. Gersabeck⁶¹, T. Gershon⁵⁵,
 D. Gerstel¹⁰, Ph. Ghez⁸, V. Gibson⁵⁴, A. Gioventù⁴⁵, O.G. Girard⁴⁸, P. Gironella Gironell⁴⁴,
 L. Giubega³⁶, C. Giugliano²⁰, K. Gizdov⁵⁷, V.V. Gligorov¹², C. Göbel⁷⁰, D. Golubkov³⁸,
 A. Golutvin^{60,77}, A. Gomes^{1,a}, P. Gorbounov^{38,6}, I.V. Gorelov³⁹, C. Gotti^{24,i}, E. Govorkova³¹,
 J.P. Grabowski¹⁶, R. Graciani Diaz⁴⁴, T. Grammatico¹², L.A. Granado Cardoso⁴⁷,
 E. Graugés⁴⁴, E. Graverini⁴⁸, G. Graziani²¹, A. Grecu³⁶, R. Greim³¹, P. Griffith²⁰, L. Grillo⁶¹,
 L. Gruber⁴⁷, B.R. Gruberg Cazon⁶², C. Gu³, E. Gushchin⁴⁰, A. Guth¹³, Yu. Guz^{43,47}, T. Gys⁴⁷,
 T. Hadavizadeh⁶², G. Haefeli⁴⁸, C. Haen⁴⁷, S.C. Haines⁵⁴, P.M. Hamilton⁶⁵, Q. Han⁷, X. Han¹⁶,
 T.H. Hancock⁶², S. Hansmann-Menzemer¹⁶, N. Harnew⁶², T. Harrison⁵⁹, R. Hart³¹, C. Hasse⁴⁷,
 M. Hatch⁴⁷, J. He⁵, M. Hecker⁶⁰, K. Heijhoff³¹, K. Heinicke¹⁴, A. Heister¹⁴, A.M. Hennequin⁴⁷,
 K. Hennessy⁵⁹, L. Henry⁴⁶, J. Heuel¹³, A. Hicheur⁶⁸, D. Hill⁶², M. Hilton⁶¹, P.H. Hopchev⁴⁸,
 J. Hu¹⁶, W. Hu⁷, W. Huang⁵, W. Hulsbergen³¹, T. Humair⁶⁰, R.J. Hunter⁵⁵, M. Hushchyn⁷⁸,
 D. Hutchcroft⁵⁹, D. Hynds³¹, P. Ibis¹⁴, M. Idzik³⁴, P. Ilten⁵², A. Inglese³⁷, A. Inyakin⁴³,
 K. Ivshin³⁷, R. Jacobsson⁴⁷, S. Jakobsen⁴⁷, E. Jans³¹, B.K. Jashal⁴⁶, A. Jawahery⁶⁵, V. Jevtic¹⁴,
 F. Jiang³, M. John⁶², D. Johnson⁴⁷, C.R. Jones⁵⁴, B. Jost⁴⁷, N. Jurik⁶², S. Kandybei⁵⁰,
 M. Karacson⁴⁷, J.M. Kariuki⁵³, N. Kazeev⁷⁸, M. Kecke¹⁶, F. Keizer^{54,54}, M. Kelsey⁶⁷,
 M. Kenzie⁵⁵, T. Ketel³², B. Khanji⁴⁷, A. Kharisova⁷⁹, K.E. Kim⁶⁷, T. Kirn¹³, V.S. Kirsebom⁴⁸,
 S. Klaver²², K. Klimaszewski³⁵, S. Koliiev⁵¹, A. Kondybayeva⁷⁷, A. Konoplyannikov³⁸,
 P. Kopciewicz³⁴, R. Kopečna¹⁶, P. Koppenburg³¹, I. Kostiuk^{31,51}, O. Kot⁵¹, S. Kotriakhova³⁷,
 L. Kravchuk⁴⁰, R.D. Krawczyk⁴⁷, M. Kreps⁵⁵, F. Kress⁶⁰, S. Kretzschmar¹³, P. Krokovny^{42,x},
 W. Krupa³⁴, W. Krzemien³⁵, W. Kucewicz^{33,l}, M. Kucharczyk³³, V. Kudryavtsev^{42,x},
 H.S. Kuindersma³¹, G.J. Kunde⁶⁶, T. Kvaratskheliya³⁸, D. Lacarrere⁴⁷, G. Lafferty⁶¹, A. Lai²⁶,
 D. Lancierini⁴⁹, J.J. Lane⁶¹, G. Lanfranchi²², C. Langenbruch¹³, T. Latham⁵⁵, F. Lazzari^{28,v},
 C. Lazzeroni⁵², R. Le Gac¹⁰, R. Lefèvre⁹, A. Leflat³⁹, O. Leroy¹⁰, T. Lesiak³³, B. Leverington¹⁶,
 H. Li⁷¹, X. Li⁶⁶, Y. Li⁶, Z. Li⁶⁷, X. Liang⁶⁷, R. Lindner⁴⁷, V. Lisovskyi¹⁴, G. Liu⁷¹, X. Liu³,
 D. Loh⁵⁵, A. Loi²⁶, J. Lomba Castro⁴⁵, I. Longstaff⁵⁸, J.H. Lopes², G. Loustau⁴⁹, G.H. Lovell⁵⁴,
 Y. Lu⁶, D. Lucchesi^{27,o}, M. Lucio Martinez³¹, Y. Luo³, A. Lupato²⁷, E. Luppi^{20,g}, O. Lupton⁵⁵,
 A. Lusiani^{28,t}, X. Lyu⁵, S. Maccolini^{19,e}, F. Machefer¹¹, F. Maciuc³⁶, V. Macko⁴⁸,
 P. Mackowiak¹⁴, S. Maddrell-Mander⁵³, L.R. Madhan Mohan⁵³, O. Maev^{37,47}, A. Maevskiy⁷⁸,
 D. Maisuzenko³⁷, M.W. Majewski³⁴, S. Malde⁶², B. Malecki⁴⁷, A. Malinin⁷⁶, T. Maltsev^{42,x},
 H. Malygina¹⁶, G. Manca^{26,f}, G. Mancinelli¹⁰, R. Manera Escalero⁴⁴, D. Manuzzi^{19,e},
 D. Marangotto^{25,q}, J. Maratas^{9,w}, J.F. Marchand⁸, U. Marconi¹⁹, S. Mariani²¹,
 C. Marin Benito¹¹, M. Marinangeli⁴⁸, P. Marino⁴⁸, J. Marks¹⁶, P.J. Marshall⁵⁹, G. Martellotti³⁰,
 L. Martinazzoli⁴⁷, M. Martinelli^{24,i}, D. Martinez Santos⁴⁵, F. Martinez Vidal⁴⁶, A. Massafferri¹,
 M. Materok¹³, R. Matev⁴⁷, A. Mathad⁴⁹, Z. Mathe⁴⁷, V. Matiunin³⁸, C. Matteuzzi²⁴,
 K.R. Mattioli⁸⁰, A. Mauri⁴⁹, E. Maurice^{11,b}, M. McCann⁶⁰, L. McConnell¹⁷, A. McNab⁶¹,
 R. McNulty¹⁷, J.V. Mead⁵⁹, B. Meadows⁶⁴, C. Meaux¹⁰, G. Meier¹⁴, N. Meinert⁷⁴,
 D. Melnychuk³⁵, S. Meloni^{24,i}, M. Merk³¹, A. Merli²⁵, M. Mikhasenko⁴⁷, D.A. Milanese⁷³,
 E. Millard⁵⁵, M.-N. Minard⁸, O. Mineev³⁸, L. Minzoni^{20,g}, S.E. Mitchell⁵⁷, B. Mitreska⁶¹,
 D.S. Mitzel⁴⁷, A. Mödden¹⁴, A. Mogini¹², R.D. Moise⁶⁰, T. Mombächer¹⁴, I.A. Monroy⁷³,
 S. Monteil⁹, M. Morandin²⁷, G. Morello²², M.J. Morello^{28,t}, J. Moron³⁴, A.B. Morris¹⁰,
 A.G. Morris⁵⁵, R. Mountain⁶⁷, H. Mu³, F. Muheim⁵⁷, M. Mukherjee⁷, M. Mulder³¹,
 D. Müller⁴⁷, K. Müller⁴⁹, V. Müller¹⁴, C.H. Murphy⁶², D. Murray⁶¹, P. Muzzetto²⁶, P. Naik⁵³,
 T. Nakada⁴⁸, R. Nandakumar⁵⁶, A. Nandi⁶², T. Nanut⁴⁸, I. Nasteva², M. Needham⁵⁷,
 N. Neri^{25,q}, S. Neubert¹⁶, N. Neufeld⁴⁷, R. Newcombe⁶⁰, T.D. Nguyen⁴⁸, C. Nguyen-Mau^{48,n},
 H. Ni⁵, E.M. Niel¹¹, S. Nieswand¹³, N. Nikitin³⁹, N.S. Nolte⁴⁷, C. Nunez⁸⁰,
 A. Oblakowska-Mucha³⁴, V. Obraztsov⁴³, S. Ogilvy⁵⁸, D.P. O'Hanlon¹⁹, R. Oldeman^{26,f},
 C.J.G. Onderwater⁷⁵, J. D. Osborn⁸⁰, A. Ossowska³³, J.M. Otalora Goicochea²,
 T. Ovsiannikova³⁸, P. Owen⁴⁹, A. Oyanguren⁴⁶, P.R. Pais⁴⁸, T. Pajero^{28,t}, A. Palano¹⁸,

M. Palutan²², G. Panshin⁷⁹, A. Papanestis⁵⁶, M. Pappagallo⁵⁷, L.L. Pappalardo^{20,g},
C. Pappenheimer⁶⁴, W. Parker⁶⁵, C. Parkes⁶¹, G. Passaleva^{21,47}, A. Pastore¹⁸, M. Patel⁶⁰,
C. Patrignani^{19,e}, A. Pearce⁴⁷, A. Pellegrino³¹, M. Pepe Altarelli⁴⁷, S. Perazzini¹⁹, D. Pereira³⁸,
P. Perret⁹, L. Pescatore⁴⁸, K. Petridis⁵³, A. Petrolini^{23,h}, A. Petrov⁷⁶, S. Petrucci⁵⁷,
M. Petruzzo^{25,q}, B. Pietrzyk⁸, G. Pietrzyk⁴⁸, M. Pili⁶², D. Pinci³⁰, J. Pinzino⁴⁷, F. Pisani⁴⁷,
A. Piucci¹⁶, V. Placinta³⁶, S. Playfer⁵⁷, J. Plews⁵², M. Plo Casasus⁴⁵, F. Polci¹²,
M. Poli Lener²², M. Poliakova⁶⁷, A. Poluektov¹⁰, N. Polukhina^{77,c}, I. Polyakov⁶⁷, E. Polycarpo²,
G.J. Pomery⁵³, S. Ponce⁴⁷, A. Popov⁴³, D. Popov⁵², S. Poslavskii⁴³, K. Prasanth³³,
L. Promberger⁴⁷, C. Prouve⁴⁵, V. Pugatch⁵¹, A. Puig Navarro⁴⁹, H. Pullen⁶², G. Punzi^{28,p},
W. Qian⁵, J. Qin⁵, R. Quagliani¹², B. Quintana⁹, N.V. Raab¹⁷, R.I. Rabadan Trejo¹⁰,
B. Rachwal³⁴, J.H. Rademacker⁵³, M. Rama²⁸, M. Ramos Pernas⁴⁵, M.S. Rangel²,
F. Ratnikov^{41,78}, G. Raven³², M. Reboud⁸, F. Redi⁴⁸, F. Reiss¹², C. Remon Alepuz⁴⁶, Z. Ren³,
V. Renaudin⁶², S. Ricciardi⁵⁶, S. Richards⁵³, K. Rinnert⁵⁹, P. Robbe¹¹, A. Robert¹²,
A.B. Rodrigues⁴⁸, E. Rodrigues⁶⁴, J.A. Rodriguez Lopez⁷³, M. Roehrken⁴⁷, S. Roiser⁴⁷,
A. Rollings⁶², V. Romanovskiy⁴³, M. Romero Lamas⁴⁵, A. Romero Vidal⁴⁵, J.D. Roth⁸⁰,
M. Rotondo²², M.S. Rudolph⁶⁷, T. Ruf⁴⁷, J. Ruiz Vidal⁴⁶, J. Ryzka³⁴, J.J. Saborido Silva⁴⁵,
N. Sagidova³⁷, B. Saitta^{26,f}, C. Sanchez Gras³¹, C. Sanchez Mayordomo⁴⁶, R. Santacesaria³⁰,
C. Santamarina Rios⁴⁵, M. Santimaria²², E. Santovetti^{29,j}, G. Sarpis⁶¹, A. Sarti³⁰,
C. Satriano^{30,s}, A. Satta²⁹, M. Saur⁵, D. Savrina^{38,39}, L.G. Scantlebury Smead⁶², S. Schael¹³,
M. Schellenberg¹⁴, M. Schiller⁵⁸, H. Schindler⁴⁷, M. Schmelling¹⁵, T. Schmelzer¹⁴, B. Schmidt⁴⁷,
O. Schneider⁴⁸, A. Schopper⁴⁷, H.F. Schreiner⁶⁴, M. Schubiger³¹, S. Schulte⁴⁸, M.H. Schune¹¹,
R. Schwemmer⁴⁷, B. Sciascia²², A. Sciubba^{30,k}, S. Sellam⁶⁸, A. Semennikov³⁸, A. Sergi^{52,47},
N. Serra⁴⁹, J. Serrano¹⁰, L. Sestini²⁷, A. Seuthe¹⁴, P. Seyfert⁴⁷, D.M. Shangase⁸⁰, M. Shapkin⁴³,
L. Shchutska⁴⁸, T. Shears⁵⁹, L. Shekhtman^{42,x}, V. Shevchenko^{76,77}, E. Shmanin⁷⁷,
J.D. Shupperd⁶⁷, B.G. Siddi²⁰, R. Silva Coutinho⁴⁹, L. Silva de Oliveira², G. Simi^{27,o},
S. Simone^{18,d}, I. Skiba²⁰, N. Skidmore¹⁶, T. Skwarnicki⁶⁷, M.W. Slater⁵², J.G. Smeaton⁵⁴,
A. Smetkina³⁸, E. Smith¹³, I.T. Smith⁵⁷, M. Smith⁶⁰, A. Snoch³¹, M. Soares¹⁹,
L. Soares Lavra¹, M.D. Sokoloff⁶⁴, F.J.P. Soler⁵⁸, B. Souza De Paula², B. Spaan¹⁴,
E. Spadaro Norella^{25,q}, P. Spradlin⁵⁸, F. Stagni⁴⁷, M. Stahl⁶⁴, S. Stahl⁴⁷, P. Steffen⁴⁸,
O. Steinkamp⁴⁹, S. Stemmler¹⁶, O. Stenyakin⁴³, M. Stepanova³⁷, H. Stevens¹⁴, S. Stone⁶⁷,
S. Stracka²⁸, M.E. Stramaglia⁴⁸, M. Straticiu³⁶, S. Strokov⁷⁹, J. Sun³, L. Sun⁷², Y. Sun⁶⁵,
P. Svihra⁶¹, K. Swientek³⁴, A. Szabelski³⁵, T. Szumlak³⁴, M. Szymanski⁵, S. Taneja⁶¹, Z. Tang³,
T. Tekampe¹⁴, G. Tellarini²⁰, F. Teubert⁴⁷, E. Thomas⁴⁷, K.A. Thomson⁵⁹, M.J. Tilley⁶⁰,
V. Tisserand⁹, S. T'Jampens⁸, M. Tobin⁶, S. Tolck⁴⁷, L. Tomassetti^{20,g}, D. Tonelli²⁸,
D. Torres Machado¹, D.Y. Tou¹², E. Tournefier⁸, M. Traill⁵⁸, M.T. Tran⁴⁸, C. Trippi⁴⁸,
A. Trisovic⁵⁴, A. Tsaregorodtsev¹⁰, G. Tuci^{28,47,p}, A. Tully⁴⁸, N. Tuning³¹, A. Ukleja³⁵,
A. Usachov¹¹, A. Ustyuzhanin^{41,78}, U. Uwer¹⁶, A. Vagner⁷⁹, V. Vagnoni¹⁹, A. Valassi⁴⁷,
G. Valenti¹⁹, M. van Beuzekom³¹, H. Van Hecke⁶⁶, E. van Herwijnen⁴⁷, C.B. Van Hulse¹⁷,
M. van Veghel⁷⁵, R. Vazquez Gomez⁴⁴, P. Vazquez Regueiro⁴⁵, C. Vázquez Sierra³¹, S. Vecchi²⁰,
J.J. Velthuis⁵³, M. Veltri^{21,r}, A. Venkateswaran⁶⁷, M. Vernet⁹, M. Veronesi³¹, M. Vesterinen⁵⁵,
J.V. Viana Barbosa⁴⁷, D. Vieira⁵, M. Vieites Diaz⁴⁸, H. Viemann⁷⁴, X. Vilasis-Cardona^{44,m},
A. Vitkovskiy³¹, V. Volkov³⁹, A. Vollhardt⁴⁹, D. Vom Bruch¹², A. Vorobyev³⁷, V. Vorobyev^{42,x},
N. Voropaev³⁷, R. Waldi⁷⁴, J. Walsh²⁸, J. Wang³, J. Wang⁷², J. Wang⁶, M. Wang³, Y. Wang⁷,
Z. Wang⁴⁹, D.R. Ward⁵⁴, H.M. Wark⁵⁹, N.K. Watson⁵², D. Websdale⁶⁰, A. Weiden⁴⁹,
C. Weisser⁶³, B.D.C. Westhenry⁵³, D.J. White⁶¹, M. Whitehead¹³, D. Wiedner¹⁴,
G. Wilkinson⁶², M. Wilkinson⁶⁷, I. Williams⁵⁴, M. Williams⁶³, M.R.J. Williams⁶¹,
T. Williams⁵², F.F. Wilson⁵⁶, W. Wislicki³⁵, M. Witek³³, L. Witola¹⁶, G. Wormser¹¹,
S.A. Wotton⁵⁴, H. Wu⁶⁷, K. Wyllie⁴⁷, Z. Xiang⁵, D. Xiao⁷, Y. Xie⁷, H. Xing⁷¹, A. Xu³, L. Xu³,
M. Xu⁷, Q. Xu⁵, Z. Xu⁸, Z. Xu⁴, Z. Yang³, Z. Yang⁶⁵, Y. Yao⁶⁷, L.E. Yeomans⁵⁹, H. Yin⁷,
J. Yu^{7,aa}, X. Yuan⁶⁷, O. Yushchenko⁴³, K.A. Zarebski⁵², M. Zavertyaev^{15,c}, M. Zdybal³³,

M. Zeng³, D. Zhang⁷, L. Zhang³, S. Zhang³, W.C. Zhang^{3,z}, Y. Zhang⁴⁷, A. Zhelezov¹⁶,
Y. Zheng⁵, X. Zhou⁵, Y. Zhou⁵, X. Zhu³, V. Zhukov^{13,39}, J.B. Zonneveld⁵⁷, S. Zucchelli^{19,e}.

¹*Centro Brasileiro de Pesquisas Físicas (CBPF), Rio de Janeiro, Brazil*

²*Universidade Federal do Rio de Janeiro (UFRJ), Rio de Janeiro, Brazil*

³*Center for High Energy Physics, Tsinghua University, Beijing, China*

⁴*School of Physics State Key Laboratory of Nuclear Physics and Technology, Peking University, Beijing, China*

⁵*University of Chinese Academy of Sciences, Beijing, China*

⁶*Institute Of High Energy Physics (IHEP), Beijing, China*

⁷*Institute of Particle Physics, Central China Normal University, Wuhan, Hubei, China*

⁸*Univ. Grenoble Alpes, Univ. Savoie Mont Blanc, CNRS, IN2P3-LAPP, Annecy, France*

⁹*Université Clermont Auvergne, CNRS/IN2P3, LPC, Clermont-Ferrand, France*

¹⁰*Aix Marseille Univ, CNRS/IN2P3, CPPM, Marseille, France*

¹¹*LAL, Univ. Paris-Sud, CNRS/IN2P3, Université Paris-Saclay, Orsay, France*

¹²*LPNHE, Sorbonne Université, Paris Diderot Sorbonne Paris Cité, CNRS/IN2P3, Paris, France*

¹³*I. Physikalisches Institut, RWTH Aachen University, Aachen, Germany*

¹⁴*Fakultät Physik, Technische Universität Dortmund, Dortmund, Germany*

¹⁵*Max-Planck-Institut für Kernphysik (MPIK), Heidelberg, Germany*

¹⁶*Physikalisches Institut, Ruprecht-Karls-Universität Heidelberg, Heidelberg, Germany*

¹⁷*School of Physics, University College Dublin, Dublin, Ireland*

¹⁸*INFN Sezione di Bari, Bari, Italy*

¹⁹*INFN Sezione di Bologna, Bologna, Italy*

²⁰*INFN Sezione di Ferrara, Ferrara, Italy*

²¹*INFN Sezione di Firenze, Firenze, Italy*

²²*INFN Laboratori Nazionali di Frascati, Frascati, Italy*

²³*INFN Sezione di Genova, Genova, Italy*

²⁴*INFN Sezione di Milano-Bicocca, Milano, Italy*

²⁵*INFN Sezione di Milano, Milano, Italy*

²⁶*INFN Sezione di Cagliari, Monserrato, Italy*

²⁷*INFN Sezione di Padova, Padova, Italy*

²⁸*INFN Sezione di Pisa, Pisa, Italy*

²⁹*INFN Sezione di Roma Tor Vergata, Roma, Italy*

³⁰*INFN Sezione di Roma La Sapienza, Roma, Italy*

³¹*Nikhef National Institute for Subatomic Physics, Amsterdam, Netherlands*

³²*Nikhef National Institute for Subatomic Physics and VU University Amsterdam, Amsterdam, Netherlands*

³³*Henryk Niewodniczanski Institute of Nuclear Physics Polish Academy of Sciences, Kraków, Poland*

³⁴*AGH - University of Science and Technology, Faculty of Physics and Applied Computer Science, Kraków, Poland*

³⁵*National Center for Nuclear Research (NCBJ), Warsaw, Poland*

³⁶*Horia Hulubei National Institute of Physics and Nuclear Engineering, Bucharest-Magurele, Romania*

³⁷*Petersburg Nuclear Physics Institute NRC Kurchatov Institute (PNPI NRC KI), Gatchina, Russia*

³⁸*Institute of Theoretical and Experimental Physics NRC Kurchatov Institute (ITEP NRC KI), Moscow, Russia, Moscow, Russia*

³⁹*Institute of Nuclear Physics, Moscow State University (SINP MSU), Moscow, Russia*

⁴⁰*Institute for Nuclear Research of the Russian Academy of Sciences (INR RAS), Moscow, Russia*

⁴¹*Yandex School of Data Analysis, Moscow, Russia*

⁴²*Budker Institute of Nuclear Physics (SB RAS), Novosibirsk, Russia*

⁴³*Institute for High Energy Physics NRC Kurchatov Institute (IHEP NRC KI), Protvino, Russia, Protvino, Russia*

⁴⁴*ICCUB, Universitat de Barcelona, Barcelona, Spain*

⁴⁵*Instituto Galego de Física de Altas Enerxías (IGFAE), Universidade de Santiago de Compostela, Santiago de Compostela, Spain*

⁴⁶*Instituto de Física Corpuscular, Centro Mixto Universidad de Valencia - CSIC, Valencia, Spain*

⁴⁷*European Organization for Nuclear Research (CERN), Geneva, Switzerland*

⁴⁸*Institute of Physics, Ecole Polytechnique Fédérale de Lausanne (EPFL), Lausanne, Switzerland*

- ⁴⁹ *Physik-Institut, Universität Zürich, Zürich, Switzerland*
- ⁵⁰ *NSC Kharkiv Institute of Physics and Technology (NSC KIPT), Kharkiv, Ukraine*
- ⁵¹ *Institute for Nuclear Research of the National Academy of Sciences (KINR), Kyiv, Ukraine*
- ⁵² *University of Birmingham, Birmingham, United Kingdom*
- ⁵³ *H.H. Wills Physics Laboratory, University of Bristol, Bristol, United Kingdom*
- ⁵⁴ *Cavendish Laboratory, University of Cambridge, Cambridge, United Kingdom*
- ⁵⁵ *Department of Physics, University of Warwick, Coventry, United Kingdom*
- ⁵⁶ *STFC Rutherford Appleton Laboratory, Didcot, United Kingdom*
- ⁵⁷ *School of Physics and Astronomy, University of Edinburgh, Edinburgh, United Kingdom*
- ⁵⁸ *School of Physics and Astronomy, University of Glasgow, Glasgow, United Kingdom*
- ⁵⁹ *Oliver Lodge Laboratory, University of Liverpool, Liverpool, United Kingdom*
- ⁶⁰ *Imperial College London, London, United Kingdom*
- ⁶¹ *Department of Physics and Astronomy, University of Manchester, Manchester, United Kingdom*
- ⁶² *Department of Physics, University of Oxford, Oxford, United Kingdom*
- ⁶³ *Massachusetts Institute of Technology, Cambridge, MA, United States*
- ⁶⁴ *University of Cincinnati, Cincinnati, OH, United States*
- ⁶⁵ *University of Maryland, College Park, MD, United States*
- ⁶⁶ *Los Alamos National Laboratory (LANL), Los Alamos, United States*
- ⁶⁷ *Syracuse University, Syracuse, NY, United States*
- ⁶⁸ *Laboratory of Mathematical and Subatomic Physics , Constantine, Algeria, associated to ²*
- ⁶⁹ *School of Physics and Astronomy, Monash University, Melbourne, Australia, associated to ⁵⁵*
- ⁷⁰ *Pontifícia Universidade Católica do Rio de Janeiro (PUC-Rio), Rio de Janeiro, Brazil, associated to ²*
- ⁷¹ *South China Normal University, Guangzhou, China, associated to ³*
- ⁷² *School of Physics and Technology, Wuhan University, Wuhan, China, associated to ³*
- ⁷³ *Departamento de Física , Universidad Nacional de Colombia, Bogota, Colombia, associated to ¹²*
- ⁷⁴ *Institut für Physik, Universität Rostock, Rostock, Germany, associated to ¹⁶*
- ⁷⁵ *Van Swinderen Institute, University of Groningen, Groningen, Netherlands, associated to ³¹*
- ⁷⁶ *National Research Centre Kurchatov Institute, Moscow, Russia, associated to ³⁸*
- ⁷⁷ *National University of Science and Technology “MISIS”, Moscow, Russia, associated to ³⁸*
- ⁷⁸ *National Research University Higher School of Economics, Moscow, Russia, associated to ⁴¹*
- ⁷⁹ *National Research Tomsk Polytechnic University, Tomsk, Russia, associated to ³⁸*
- ⁸⁰ *University of Michigan, Ann Arbor, United States, associated to ⁶⁷*

^a *Universidade Federal do Triângulo Mineiro (UFMT), Uberaba-MG, Brazil*

^b *Laboratoire Leprince-Ringuet, Palaiseau, France*

^c *P.N. Lebedev Physical Institute, Russian Academy of Science (LPI RAS), Moscow, Russia*

^d *Università di Bari, Bari, Italy*

^e *Università di Bologna, Bologna, Italy*

^f *Università di Cagliari, Cagliari, Italy*

^g *Università di Ferrara, Ferrara, Italy*

^h *Università di Genova, Genova, Italy*

ⁱ *Università di Milano Bicocca, Milano, Italy*

^j *Università di Roma Tor Vergata, Roma, Italy*

^k *Università di Roma La Sapienza, Roma, Italy*

^l *AGH - University of Science and Technology, Faculty of Computer Science, Electronics and Telecommunications, Kraków, Poland*

^m *LIFAELS, La Salle, Universitat Ramon Llull, Barcelona, Spain*

ⁿ *Hanoi University of Science, Hanoi, Vietnam*

^o *Università di Padova, Padova, Italy*

^p *Università di Pisa, Pisa, Italy*

^q *Università degli Studi di Milano, Milano, Italy*

^r *Università di Urbino, Urbino, Italy*

^s *Università della Basilicata, Potenza, Italy*

^t *Scuola Normale Superiore, Pisa, Italy*

^u *Università di Modena e Reggio Emilia, Modena, Italy*

^v *Università di Siena, Siena, Italy*

^w *MSU - Iligan Institute of Technology (MSU-IIT), Iligan, Philippines*

^x*Novosibirsk State University, Novosibirsk, Russia*

^y*INFN Sezione di Trieste, Trieste, Italy*

^z*School of Physics and Information Technology, Shaanxi Normal University (SNNU), Xi'an, China*

^{aa}*Physics and Micro Electronic College, Hunan University, Changsha City, China*

[†]*Deceased*